11-1-2022

Vitamin e Does Not Disturb Polyunsaturated Fatty Acid Lipid Domains

Mitchell Dipasquale
University of Windsor

Michael H.L. Nguyen
University of Windsor

Stuart R. Castillo
University of Windsor

Isabelle J. Dib
University of Windsor

Elizabeth G. Kelley
NIST Center for Neutron Research

See next page for additional authors

Vitamin E Does Not Disturb Polyunsaturated Fatty Acid Lipid Domains

Mitchell DiPasquale,[†] Michael H. L. Nguyen,[†] Stuart R. Castillo,[†] Isabelle J. Dib,[†] Elizabeth G. Kelley,[‡] and Drew Marquardt[*,†,¶]

[†]*Department of Chemistry and Biochemistry, University of Windsor, Windsor, Ontario, Canada*

[‡]*NIST Center for Neutron Research, National Institute of Standards and Technology, Gaithersburg, Maryland, USA*

[¶]*Department of Physics, University of Windsor, Windsor, Ontario, Canada*

E-mail: drew.marquardt@uwindsor.ca

Abstract

The function of vitamin E in biomembranes remains a prominent topic of discussion. As its limitations as an antioxidant persist and novel functions are discovered, our understanding of the role of vitamin E becomes increasingly enigmatic. As a group of lipophilic molecules (tocopherols and tocotrienols), vitamin E has been shown to influence the properties of its host membrane, and a wealth of research has connected vitamin E to polyunsaturated fatty acid (PUFA) lipids. Here, we use contrast-matched small angle neutron scattering and differential scanning calorimetry to integrate these fields by examining the influence of vitamin E on lipid domain stability in PUFA-based lipid mixtures. The influence of α-tocopherol, γ-tocopherol, and α-tocopherylquinone on the lateral organization of a 1:1 lipid mixture of saturated distearoylphosphatidylcholine (DSPC) and polyunsaturated palmitoyl-linoleoylphosphatidylcholine (PLiPC)

with cholesterol provides a complement to our growing understanding of the influence of tocopherol on lipid phases. Characterization of domain melting suggests a slight depression in the transition temperature and a decrease in transition cooperativity. Tocopherol concentrations that are an order of magnitude higher than anticipated physiological concentrations (2 mole percent) do not significantly perturb lipid domains; however, addition of 10 mole percent is able to destabilize domains and promote lipid mixing. In contrast to this behaviour, increasing concentrations of the oxidized product of α-tocopherol (α-tocopherylquinone) induces a proportional increase in domain stabilization. We speculate how the contrasting effect of the oxidized product may supplement the antioxidant response of vitamin E.

Introduction

A century ago, Evans and Bishop identified vitamin E as a vital dietary nutrient for mammalian reproduction.[1] Now, vitamin E is known to be a collective of eight molecular tocol species: including tocopherols and tocotrienols, with an expanse of biological and biophysical significance.[2–5] Tocopherols are the more abundant subgroup of the family, which structurally vary by methyl substituents on the chromanol ring as illustrated by Fig. 1A. Though this variation is considerably discreet, it is remarkable that only α-tocopherol (αToc) is actively retained by the human body, in spite of the fact that other forms (γ-tocopherol, γToc) are more naturally abundant.[6–8]

Vitamin E is widely recognized as a potent lipid-soluble antioxidant serving to protect cell membranes from irreversible oxidative damage.[3,9–13] The presence of oxidation-sensitive polyunsaturated fatty acid (PUFA) lipids is accompanied by increased levels of vitamin E, and work has presumed an affinity of vitamin E for these disordered environments.[14–17] Neutron diffraction studies of αToc in lipid bilayers have confirmed a depth just below the membrane interface and orientation that coincides with an antioxidant function.[13,18–20] From this position, oxidized tocopherol can be recycled by more abundant aqueous antioxidants,

A. Tocopherol

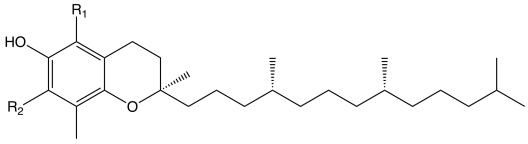

Structure	R_1	R_2
α-tocopherol (αToc)	CH_3	CH_3
β-tocopherol	CH_3	H

Structure	R_1	R_2
γ-tocopherol (γToc)	H	CH_3
δ-tocopherol	H	H

B. α-Tocopherylquinone

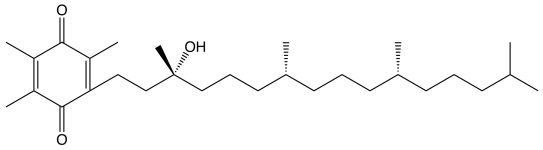

C. PLiPC

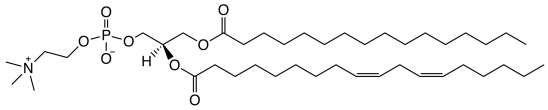

D. DSPC

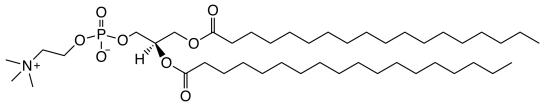

Figure 1: Structures of tocopherol and lipid species. In this work, we explore the tocopherol species (**A**) α-tocopherol, the species preferentially absorbed by the human body; γ-tocopherol, the most naturally abundant species; and (**B**) α-tocopherylquinone, the stable oxidation product of αToc in a system composed of the low-melting PUFA lipid (**C**) palmitoyl-linoleoylphosphatidylcholine and high-melting lipid (**D**) distearoylphosphatidylcholine.

or terminated as α-tocopherylquinone (αTocQ, Fig. 1B).[21] A wealth of research endorses an antioxidant role of vitamin E; yet, a lack of *in vivo* evidence and perplexingly low physiological abundance raises concerns about the ability of vitamin E to be effective as the membrane's front-line defence against oxidation.[5,22–24]

The biological selectivity for one tocopherol variety incites suspicion that tocopherol has a physiological significance beyond oxidation protection; in fact, other tocols are notably more efficient antioxidants.[25] This speculation has fueled clinical reports on vitamin E describing a vast array of roles from immunity,[26] to cardiovascular health[27] and anti-cancer activities,[28] though often accompanied by little mechanistic detail and muddled in controversy.[4,5,22,23] Of the more notable clinical discoveries, a body of work correlates excessive supplementation of

vitamin E to an increased risk of developing prostate cancer in healthy men.[29–31]

Interestingly, in many cases of prostate cancer, cell membranes present excess cholesterol and caveolae-type nanoscale lipid rafts.[32] This observation implies cancer proliferation through an abundance of cholesterol-rich liquid-ordered L_o domains that serve as platforms to functionalize the membrane surface.[33–35] In line with this theory, studies have shown that modifying the cellular lipidome by supplementation of polyunsaturated fatty acids (PUFAs) can suppress prostate tumor growth by a variety of mechanisms.[36–38] However, the dietary requirement of αToc also increases proportionally with PUFA consumption, which further complicates observations at the membrane-level.[14]

In our previous work, we began to define the effects of vitamin E species on the organization, and thereby functionalization, of cell membranes using an established model membrane platform.[39] Large hemispherical L_o domains (1:1 dipalmitoylphosphatidylcholine: dioleoylphosphatidylcholine with $\chi_{Chol} = 0.25$) are favoured by high line tension produced from demixing of homoacyl lipids. These domains were not measurably influenced by a tocopherol concentration five times greater than expected in physiology.[24] At even greater concentrations ($\approx 10 - 100$ times physiological), domain destabilization was observed, which may agree with literature that suggests an association of αToc with domain boundaries to minimize line tension.[40–42]

Though our observation of domain destablilization occurred under non-physiological conditions, it is particularly interesting that an array of studies have demonstrated a strongly contrasting effect of αToc on domain stability in response to membrane oxidation. Induction of lipid peroxidation and the consequent presence of oxidized lipids strongly induce formation of cholesterol-rich lipid domains.[43–45] These antagonistic influences on membrane organization inspires a hypothesis that membrane lateral organization provides an additional dimension to an antioxidant mechanism for vitamin E.

In this work, we expand on the relationship between tocopherol and oxidation-sensitive membrane environments by exploring the role of tocopherols on the organization of coexisting

PUFA lipid domains. Physiological membrane rafts are proposed to be nanoscopic and transient, which suggests low energetic barriers for their formation and disassembly.[46–49] While we cannot capture the transient nature of domains in our thermodynamically stable model systems, here we extend our studies to a three-component lipid composition with a low-melting hybrid acyl PUFA lipid which favours smaller and less robust domains when compared to our previous work.[39,40,50] Using contrast-matched small angle neutron scattering, we report on changes in lipid clustering induced by the addition of αToc, γToc, and α-tocopherylquinone (αTocQ) in a mixture of the PUFA-lipid palmitoyl-linoleoylphosphocholine (PLiPC, Fig. 1C) with the high-melting lipid disteraroylphosphocholine (DSPC, Fig. 1D) and cholesterol.

Materials and Methods

Materials

The lipids 1,2-distearoyl-*sn*-glycero-3-phosphocholine (18:0/18:0 PC, DSPC), 1,2-distearoyl-d70-*sn*-glycero-3-phosphocholine (18:0[d35]/18:0[d35] PC, d70-DSPC), and 1-palmitoyl-2-linoleoyl-*sn*-glycero-3-phosphocholine (16:0/18:2 PC, PLiPC) and probes 1,2-dioleoyl-*sn*-glycero-3-phosphoethanolamine-N-(lissamine rhodamine B sulfonyl) ammonium salt (LR-DOPE) and 1-palmitoyl-2-(dipyrromethene boron difluoride)undecanoyl-*sn*-glycero-3-phosphocholine (TopFluor-PC) were purchased from Avanti Polar Lipids, Inc. (Alabaster, AL). Naphtho-[2,3-a]pyrene (naphthopyrene) was purchased from TCI America (Portland, OR). Cholesterol, D-α-tocopherol (α-tocopherol, αToc), (R,R,R)-γ-tocopherol (γ-tocopherol, γToc), D-α-tocopherylquinone (α-tocopherylquinone, αTocQ) and all unspecified reagents (ACS grade) were purchased from Sigma-Aldrich (St. Louis, MO). D_2O (99.9 %) was purchased from Cambridge Isotopes (Andover, MA) and ultrapure H_2O (18.2 MΩcm) was from a Milli-Q water purification system (Millipore-Sigma, Oakville, ON). All lipids were prepared as stock solutions in chloroform and used without further purification.

Preparation of Lipid Dispersions

All samples were prepared with careful attention to maintain an inert environment of argon gas, with the majority of the work being carried out in a glove bag doubly-purged with argon or a benchtop glove box maintained below 2 % O_2. All samples were prepared from a chloroform stock solution of the lipid mixture to ensure all samples maintained a uniform lipid ratio. Periodically, thin layer chromatography was used to assess the viability of the stock solution. Chloroform was evaporated *in vacuo* for approximately 12 hours. The vacuum was interrupted by a controlled flow of argon gas to saturate the chamber prior to removing the dried lipid films. The resulting lipid films were hydrated to a concentration of 20 mg/ml using ultrapure water that had been degassed by sonication under reduced pressure, and warmed to 60 °C. For SANS sample preparations, a stoichiometric mixture of 34.6 % D_2O in H_2O was used to achieve a contrast match. Samples were sealed with the headspace purged with argon. Vesicles were permitted to swell for 30 minutes in a 50 °C water bath prior to aggressive vortexing to produce a multilamellar vesicle (MLV) suspension. The MLVs were subsequently subjected to five freeze-thaw-vortex cycles between - 80 °C and 60 °C.

For DSC measurements, the multilamellar samples were diluted to 10 mg/ml. SANS samples were processed into unilamellar vesicles (ULVs) by 31 passes through a hand-held miniextruder (Avanti Polar Lipids, Inc.) equipped with a 50 nm pore-diameter polycarbonate filter and heated to 50 °C. Samples remained sealed and were gradually cooled to room temperature prior to measurement.

For FRET measurements, samples were prepared in glass culture tubes directly from the chloroform mixture using a modified rapid solvent exchange (RSE) protocol.[51] Samples received a fixed volume of a chloroform master mix of fluorescent probes using a repeating dispenser (Hamilton, USA, Reno, NV). This controlled probe/lipid ratios at 1:200 for naphthopyrene, 1:1500 for TopFluor-PC, and 1:1500 for LR-DOPE. The RSE protocol produced a 625 μmol/L solution of vesicles without desolvation.

Förster Resonance Energy Transfer

Sample was diluted 10x with degassed water and loaded into a 1 cm path-length quartz cuvette purged with argon gas. Temperature-dependent spectra were collected using a T-geometry FLS1000 fluorometer equipped with a thermoelectrically controlled 4-window cuvette holder that was regulated within 0.1 °C by a circulating water bath (Edinburgh Instruments Ltd., Livingston, UK). Probes were excited with non-polarized light from a 450 W xenon lamp and emitted light was collected orthogonally by a PMT-900 detector. The following excitation/emission (λ, nm) channels were collected (2 nm bandpass and 0.5 s integration):

naphthopyrene fluorescence (407/470)

TopFluor-PC sensitized emission (407/520)

TopFluor-PC fluorescence (498/510)

LR-DOPE sensitized emission (498/590)

LR-DOPE fluorescence (560/590)

Data were measured in 2 °C increments in the range of 10 °C – 60 °C with equilibration of 120 s at each temperature. Sensitized acceptor emission (SAE) FRET signals were corrected for variable donor and acceptor fluorescence intensities according to Eq. 1:

$$FRET = \frac{F_{SAE}}{\sqrt{F_D \cdot F_A}} \tag{1}$$

where F_{SAE}, F_D, and F_A are the fluorescence intensities from the SAE, donor, and acceptor channels, respectively.[50] The Förster distance (R_0) of these probe pairs considered as $\approx$ 4.4 nm for naphthopyrene/TopFluor-PC (Frederick A. Heberle, personal communication) and $\approx$ 2 nm for TopFluor-PC/LR-DOPE.[52] The resulting FRET signals were normalized within the sample with the assumption of complete miscibility, and thereby a maximum or minimum SAE, at 60 °C.

Differential Scanning Calorimetry

MLV suspensions were loaded into a Nano Differential Scanning Calorimeter (TA Instruments, Waters LLC, New Castle, DE) with degassed water as the reference capillary. Alternating heating and cooling scans at a rate of 2 °C/min then 1 °C/min were conducted to equilibrate the sample. Data were collected at a rate of 0.2 °C/min in the range of 10 °C to 55 °C with isothermal holds at each end of the scan. Only the slow scan was used for analysis. Background was subtracted as a second order polynomial using the NanoAnalyze software. Data were exported and analyzed by the model-free tangent construction method using Origin(Pro) software (OriginLab Corporation, Northampton, MA).[52,53] Error in the tangential fits yields a 0.2 °C error for peak midpoint and 2 °C error for onset and endpoint estimation due to variance in the background. Both heating and cooling scans were analyzed and results were averaged to estimate thermal events.

Contrast Matched Small-Angle Neutron Scattering

For contrast matched neutron scattering investigations of lateral lipid organization, the scattering length density of the system must be tuned to suppress scattering from non-lateral features.[54,55] In this study, samples were prepared using a combination of chain protiated and chain perdeuterated (d70) DSPC such that the average scattering length density of the hydrocarbon region of the bilayer is equal to the scattering length density of the phosphatidylcholine headgroups. As per Heberle et al., suspending a contrast matched composition in mixtures of D_2O and H_2O can mask scattering from structural features that would normally dominate the scattering form factor.[40,55,56] In this situation, an increase in scattering emanates from contrast provided by lateral clustering of deuterated saturated lipid into ordered domains.

The neutron scattering experiments in this work were conducted at the Very Small- Angle Neutron Scattering (NG3-VSANS) instrument located at the National Institute of Standards and Technology Center for Neutron Research (NIST-CNR).[57] Data were acquired in the

scattering vector range of 0.009 Å^{-1} < q < 0.5 Å^{-1} using two detector carriages positioned at sample-to-detector distances of 5.4 m and 13 m. Given the oxidation sensitive nature of the samples, the instrument was configured to use a "white beam" of wavelength 5.3 Å and $\Delta\lambda/\lambda$ = 40 %. As established in our previous works, a large wavelength spread reduces q-resolution, but produces a significant increase in neutron flux, allowing for good-quality data acquisition in as little as three minutes.[39,58]

In a glove bag flush with nitrogen, vesicle suspensions at 20 mg/ml were loaded into 1 mm path-length quartz banjo cells (Hellma, USA, Plainsview, NY) capped with a Teflon plug and sealed with Parafilm. The cells were mounted in an aluminium Peltier-controlled cell holder with ≈ 1 °C accuracy and measured at seven to ten temperature points starting at 5 °C and increasing to 55 °C. At the highest temperature, the membranes should be homogeneously mixed resulting in minimum scattering, whereas lower temperature would display an increase in scattering from demixing of lipids into domain. Samples were permitted to thermally equilibrate at each temperature for approximately 18 minutes prior to measurement. A subsequent set of measurements using course temperature-step in the cooling direction were used to assess hysteresis and potential sample oxidation.

Data were reduced, stitched, and corrected for detector pixel sensitivity, dark current, sample transmission, and background scattering using the VSANS macro on Igor Pro provided by NIST-CNR.[59] Data were analyzed using Python scripts constructed by M. H. L. Nguyen to replicate the analysis in our previous work.[39] In brief, data were background corrected and described as model-independent quantities by extraction of the Porod invariant as in Eq. 2.[60]

$$Q = \int_0^\infty q^2 I(q) dq \tag{2}$$

The Porod invariant Q quantifies the total scattering from the sample, which under our contrast matched conditions is dependent on the extent to which protiated and deuterated lipid cluster. Error in measurement was determined by repeating the analysis using simulated

data formed by the upper and lower limits defined by the form factor error bars. For all samples, standard error was less than 1%. To a first approximation described in Eq. 3, the extent of scattering can be correlated to the area fraction of the ordered phase a_{L_o} and the contrast $\Delta\rho$ between the ordered phase and the bulk.[61]

$$Q \approx a_{L_o}(1 - a_{L_o})\Delta\rho^2 \tag{3}$$

Under these contrast matching conditions, an increase (or decrease) in Q corresponds to stabilization (destabilization) of L_o domains. Data were normalized to a range bounded by the lowest contrast condition (highest temperature) and the highest contrast condition of the system in the absence of tocopherol (lowest temperature of DSPC/PLiPC/Chol 39/39/22). In essence, this scale describes the extent of phase separation compared to the undoped system as a reference scale to qualify if a dopant is promoting or obstructing phase separation.

A simple logistic function Eq. 4 was used to relate the contrast decay with temperature.

$$Q = \frac{Q_{max}}{1 + (\frac{T}{T_m})^r} \tag{4}$$

The upper asymptote Q_{max} defines the relative highest contrast achieved, with T_m as the melting point inflection of the curve. As such, T_m indicates the temperature at which approximately half of the lipid clustering is abolished. The decay rate r accounts for a range of thermodynamic parameters that dictate the breadth of the melting process such as cooperativity and enthalpy. These parameters are derived from non-calorimetric means, and should not be taken as thermodynamic absolutes, but rather as a means to qualitatively compare the perturbation of different tocopherol species in this work.

Results and Discussion

Motivation for Experimental Design

Raft-like domains are often mimicked by three-component mixtures of lipids comprising a high-melting lipid, a low-melting lipid, and cholesterol. To satisfy the contrast-matching requirements of this neutron study, it is necessary that the phospholipid components have the same headgroup, which in our case are zwitterionic phosphatidylcholines (PC). To the best of our knowledge, at this time there is an absence of literature describing the phase behaviour of any three-component domain-forming mixture including polyunsaturated fatty acyl lipids and phosphatidylcholines. The nearest description of such a system by Konyakhina and Feigenson is not suitable as it includes a sphingomyelin high-melting lipid which would provide additional radial contributions to scattering.[62] Based on intuition from work investigating the effect of chain unsaturation and hydrophobic mismatch on phase behaviour,[40,50,63–65] we propose a composition of DSPC/PLiPC/Chol at a stoichiometry of 39/39/22 to produce nanoscale L_o/L_d coexistence. This mixture provides phosphatidylcholine headgroups to simplify neutron contrast-matching, and the single 18:2 linoleoyl polyunsaturated acyl chain is relatively resistant to oxidation in comparison to more conjugated PUFAs. This stability is particularly valuable given the constraints of neutron scattering sample environments.

Establishing the phase behaviour of DSPC/PLiPC/Chol by FRET

FRET was used to evaluate the temperature-dependent lateral organization of the base composition to validate the presence of two-phase coexistence. FRET efficiencies were measured along a heating trajectory to detect changes in the distribution of probe proximities and therefore, due to differences in partitioning, to report on the mixing behaviour of the lipids.[52,66] Two combinations of probes in low concentrations were chosen to report on the presence of L_o and L_d phases by exciting the donor.[67]

First, a FRET pair with similar phase partitioning behaviour was explored. TopFluor-PC

and LR-DOPE both preferentially partition into the PUFA-rich L_d phase, and as such FRET efficiency decreases with increasing temperature as the exclusive ordered domains melt and the area fraction of the disordered phase extends across the bilayer surface. In complement, a second pairing of naphthopyrene to TopFluor-PC produces a reciprocal result. In this case, naphthopyrene partially partitions into DSPC- and Chol-rich L_o phases and is therefore spatially isolated from the TopFluor-PC acceptor. This separation provides a reduction in FRET efficiency when the average donor-acceptor proximity is greater than the FRET pair Förster distance (R_0). Upon heating, ordered domains melt and naphthopyrene is released into the continuous phase and therefore FRET efficiency increases as a greater proportion of the naphthopyrene donor infiltrates R_0 and interacts with the TopFluor-PC acceptor.

Figure 2 shows changes in FRET efficiency as a function of temperature. At low temperatures, FRET efficiency between two probes that partition into the same lipid environment is high, and gradually tapers to a plateau at $\approx$ 46 °C (Fig. 2, ◯). This steady decline in FRET is a result of rapid lateral diffusion in the disordered phase resulting in collisional quenching, which reaches a minimum when the fluorphores are maximally dispersed along the membrane surface (the absence of domains). In contrast, probes with opposing phase preference have a low FRET efficiency at low temperatures (Fig. 2, ×), which gradually increases as the sample is heated. The miscibility gap closes with a plateau of normalized fluorescence beyond $\approx$ 46 °C, indicating that minimal phase separation beyond R_0 persists and the membrane in uniformly mixed. The naphthopyrene and TopFluor-PC probe combination, in which R_0 is approximately 4.4 nm, establishes a lower limit of domain detection. In DSPC/PLiPC/Chol at a stoichiometry of 39/39/22, the change in L_o-L_d FRET efficiency indicates the presence of ordered domains with dimensions greater than this lengthscale.

DSC indicates suppression of the phase transitions

Differential scanning calorimetry (DSC) was used to explore the thermotropic mixing behaviour of the DSPC/PLiPC/Chol composition. As illustrated in Fig. 3 (black curve), a

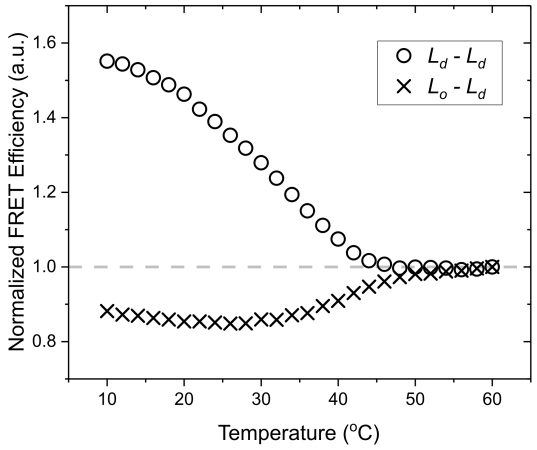

Figure 2: Temperature-dependent FRET studies on DSPC/PLiPC/Chol indicates changes in lateral organization with temperature. Probes that partition similarly into disordered phases, TopFluor-PC and LR-DOPE, exhibit a reduced FRET efficiency with increasing temperature (L_d-L_d; ◯) while probes with differing phase preference, naphthopyrene and TopFluor-PC, reflect an increase in FRET efficiency with temperature (L_o-L_d; ×). A horizontal grey dashed line denotes uniform mixing, and the miscibility gap closes as FRET efficiency of both probe pairs ceases to change beyond ≈ 46 °C.

broad peak centered at approximately 38 °C ($T_{onset/endset}$ ≈ 26–45 °C) indicates the transition of this lipid mixture into a uniform phase. Given that DSPC presents a main $L_\beta \rightarrow L_\alpha$ transition in the range ≈ 55 °C,[68] the observed broadening and depression in melting transition is anticipated when mixed with intermediate concentrations of cholesterol and low-melting lipid. The location and breadth of the observed melting transition is consistent with calorimetric and non-calorimetric measurements in similar DSPC-containing lipid compositions.[40,69] Moreover, the observed transition is consistent with the mixing event detected by FRET in Figure 2.

With the addition of $\chi = 0.02$ α- or γToc, the transition appears relatively unchanged, but depressed to lower temperatures (≈ 31 °C, traces provided in Fig. S1 of the SI). With the addition of $\chi = 0.10$ of these tocopherols, the transition is abolished beyond detection, indicating significant fluidization of the bilayer. This increase in disorder of lipid packing, and thus decrease in enthalpy and cooperativity of the transition is qualitatively consistent with previous calorimetric studies on tocopherol in a range of cholesterol-free lipid compo-

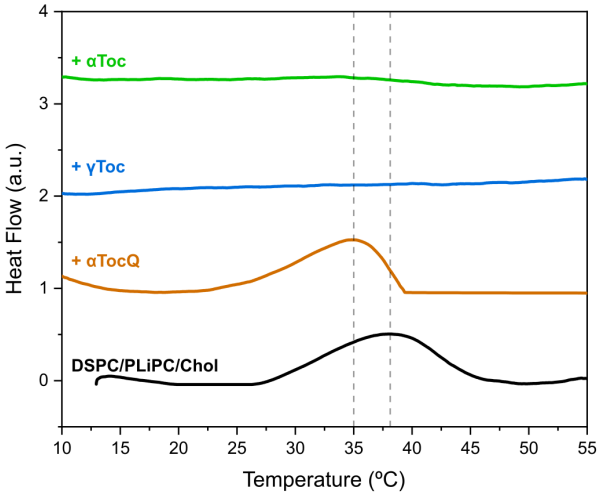

Figure 3: Differential scanning calorimetry thermograms of DSPC/PLiPC/Chol (39/39/22) (black) with the addition of $\chi = 0.10$ αToc (green), γToc (blue), or αTocQ (orange). The melting transition is abolished upon the addition of αToc or γToc, but the transition becomes more distinct in the presence of αTocQ. Determined by the tangent method, vertical dashed lines transect the melting midpoints to highlight the melting point depression induced by αTocQ. Data are collected in the heating trajectory and are vertically offset for visibility.

sitions.[70–73] In fact, the ability of tocopherol to disrupt the transition is similar to that of cholesterol, though tocopherol appears to be more effective at lower concentrations.[70,74]

In contrary, addition of αTocQ produces a transition with features reminiscent of the tocopherol-free composition, but is displaced to slightly lower temperatures (Fig. 3; orange curve). The melting transition midpoint is depressed to $\approx$ 36 °C while the breadth of the transition remains fairly consistent ($T_{onset/endset} \approx$ 23–40 °C). This observation hints that while coexisting phases persist, there is a distinct role of αTocQ to influence lipid mixing and thus the resulting phases may not be compositionally or geometrically the same.

SANS probes nanoscale lipid organization

To explore the effect of tocopherol on PUFA nanodomains in the absence of fluorescent probes, low q-resolution contrast-matched SANS was used to characterize lateral organization. As identified in previous work,[39,58] increasing the wavelength spread of the incident neutrons provides a significant reduction in acquisition time at the expense of spatial

resolution. Though structural information is compromised, total scattering information is conserved and can rapidly inform on clustering of saturated lipids into L_o domains. For greater detail on the employed contrast-matching scheme or neutron theory, please refer to the Methods section and the works of Pencer et al..[54,61]

As seen in Fig. 4A, low q-resolution neutron form factors from DSPC/PLiPC/Chol samples exhibit a suppression in scattering intensity as temperature is increased. This trend is consistent with thermally driven mixing of protiated L_d and deuterated L_o lipid phases, which we define as domain melting. This melting behaviour is qualitatively consistent with the transitions observed by FRET and DSC (Fig. 2 and 3). With the addition of $\chi = 0.10$ α- or γ-tocopherol, scattering is greatly reduced and appears irrespective of the dopant species (Fig. 4C/D). In contrast, Fig. 4B demonstrates a dramatic increase in scattering intensity when the oxidized product αTocQ is introduced. Plots in Fig.4 omit data for clarity, the full suit of form factors is provided in Fig. S2 of the SI.

For a relative quantification of the effects of each of these dopants, the Porod invariant, Q, was calculated from the reduced neutron data and normalized to the Q of the non-doped lipid mixture at 5 °C. Porod invariants before the normalization procedure can be found in Section S3 of the SI. In this case, we choose to assign a value of 1 to our base composition at 5 °C. This point represents the maximum amount of scattering, or the greatest degree of phase separation, in the absence of a vitamin E dopant. All samples are measured at 55 °C, which is above the mixing temperatures for DSPC-containing compositions, and so this point is set as zero where the membrane is laterally homogeneous and scattering emanating from lipid clustering is minimal.[40] Extracted Porod invariants are displayed in Fig. 5 as a function of temperature with the addition of $\chi = 0.02$, 0.05, or 0.1 of each αToc, γToc, and αTocQ.

In this plot style, a black boundary line is formed by the DSPC/PLiPC/Chol system. Above this line, samples scatter greater than the control system and are said to have stabilized domains, or that the dopant promotes phase separation by increasing the area fraction

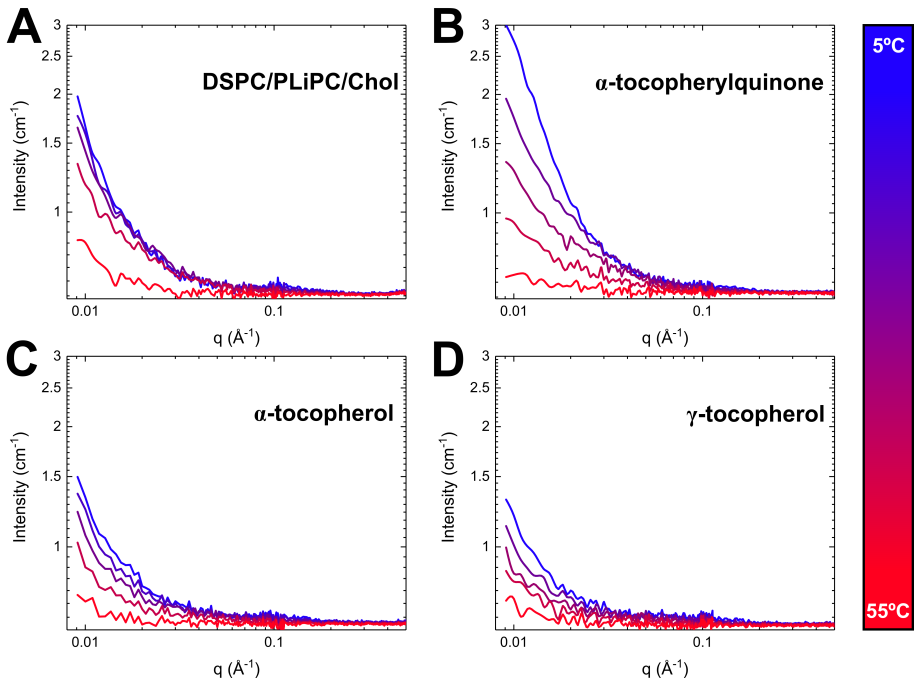

Figure 4: Low q-resolution SANS form factors demonstrate domain melting corresponding to an increase in temperature for DSPC/PLiPC/Chol in the absence of vitamin E (**A**) or with χ = 0.10 (**B**) α-tocopherylquinone, (**C**) α-tocopherol, or (**D**) γ-tocopherol. The gradient from blue to red correlates to temperature, with significant scattering at 5 °C that is abolished upon heating to 55°C. Form factors at alternating temperatures are omitted to reduce data density and improve clarity.

or homogeneity of domains. Alternatively, measurements below this line (shaded grey area) scatter less and therefore have destabilized domains, or less lateral heterogeneity, by our definition. It is important to note that this method can not decouple the source of variances in scattering. For example, Equation 3 indicates that an increase in scattering can arise from larger domains and/or an increase in contrast between the two phases; both of which we define as features of stabilized domains.

Figure 5 much more evidently displays that 10 mole percent addition of tocopherol (α or γ) is destabilizing to phase separation. This result is not exceedingly clear by DSC as coexisting phases are not sufficiently distinct to detect the heat of the mixing transition. In fact, there is a notably discontinuity between lipid phase melting (observed by DSC) and lipid miscibility (observed here by FRET and SANS). It must be noted that the absence of a phase

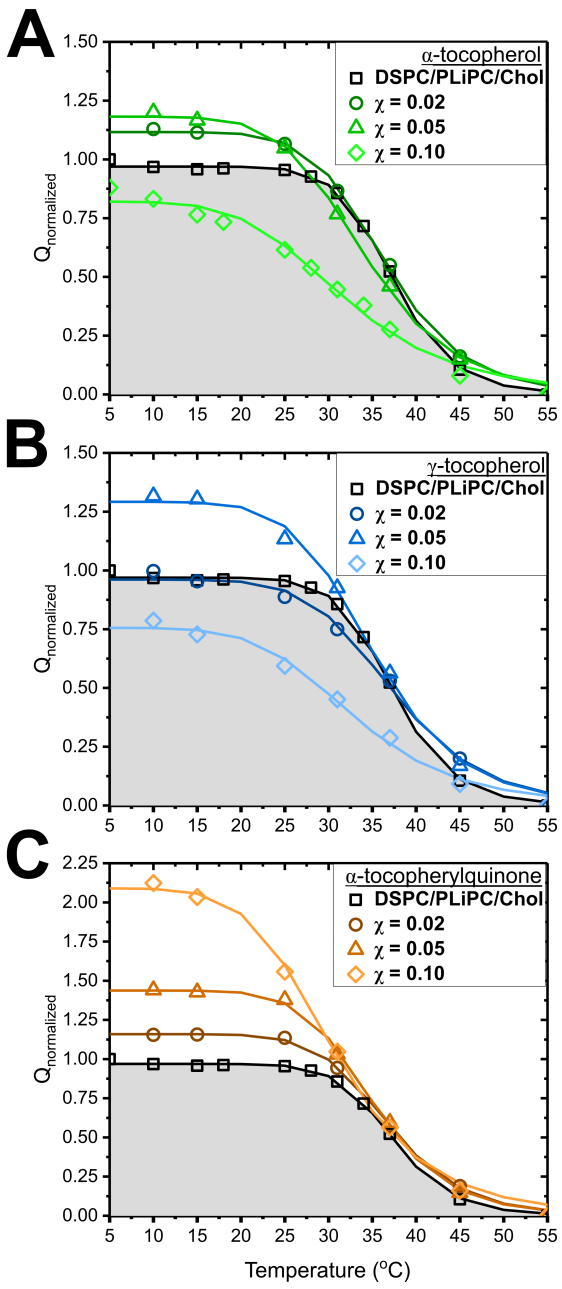

Figure 5: Normalized scattering intensity $Q_{normalized}$ of domain melting derived from SANS. DSPC/PLiPC/Chol in the absence of vitamin E (□; black) defines the boundary above which domains are said to be stabilized and below (shaded grey) are described as destabilized. The base composition is doped with the vitamin E species (**A**) α-tocopherol (green), (**B**) γ-tocopherol (blue), or (**C**) α-tocopherylquinone (orange) at mole fractions $\chi = 0.02$ (◯), $\chi = 0.05$ (△), and $\chi = 0.10$ (◊). Solid lines are best fits of a simple logistic function in Eq. 4 to the data to characterize the melting behaviour of the systems. The standard deviation is $< 1\%$ and the error bars are smaller than the markers.

transition by DSC does not necessarily indicate lipid miscibility at that temperature.[52,69,75] Interestingly, slightly different trends are observed when comparing the influence of low concentrations (χ= 0.02) of αToc and γToc —two species that differ only by a single methyl substituent. Moreover, the addition of αTocQ clearly promotes phase separation.

Characterization of domain melting using SANS

The shape of the relationships in Fig. 5 are conducive to a logistic regression to characterize the melting behaviour of the sample. Essentially, we observe neutron scattering intensity Q as a measurable quantity to report on the melting process. An analogous strategy has been used to quantify DNA melting from normalized fluorescence intensity.[76] Using the logistic function defined in Eq.4, we determine a maximum scattering intensity Q_{max}, melting temperature T_m (based on the inflection), and r as an umbrella parameter to define the melting behaviour. In the context of this process, the rate parameter r largely captures cooperativity that dictates the breadth of the transition, but due to the crudeness of the model, r encompasses a range of thermodynamic features. The fit results are summarized in Table 1.

Table 1: Parameters of logistic regressions to the Porod decay plots in Figure 5 by Equation 4 to describe the melting behaviour of the DSPC/PLiPC/Chol base composition as perturbed by vitamin E. Standard error in Q_{max} is on the order of 5 % and the accuracy in T_m is constrained by instrumental limitations at ± 1 °C. Error bars on r represent standard error.

Composition	$\mathbf{Q}_{max}$	$\mathbf{T}_m$ **(°C)**	r
DSPC/PLiPC/Chol	0.97	37	11 ± 0.5
+ α-tocopherol			
χ = 0.02	1.12	37	8 ± 0.6
χ = 0.05	1.18	34	7 ± 0.5
χ = 0.10	0.82	32	5 ± 0.6
+ γ-tocopherol			
χ = 0.02	0.96	37	7 ± 0.9
χ = 0.05	1.29	35	7 ± 0.7
χ = 0.10	0.76	33	6 ± 0.8
+ α-tocopherylquinone			
χ = 0.02	1.16	37	9 ± 0.5
χ = 0.05	1.44	35	8 ± 0.6
χ = 0.10	2.09	31	6 ± 0.5

The coefficients of determination for all fits were > 0.98.

Parameterizing the melting behaviour permits a closer comparison of vitamin E species in terms of their ability to promote or impede phase separation. For example, the maximum total scattering parameter Q_{max} describes a greater than 10 % increase in the degree of phase separation with the addition of 2 mole percent αToc. This effect is not observed with γToc, which appears to have no influence at low concentrations. Moreover, αToc and γToc appear to have a similar effect on the membrane: a slight promotion of phase separation at low concentrations which reaches a saturation and begins to hinder domains between 5-10 mole percent. These trends are well within the same magnitude, and particularly Q_{max} of systems demonstrate that high concentrations (χ=0.1) of tocopherol tend toward approximately 80 % of scattering of the undoped system.

Addition of αTocQ provides a unique trend of domain stabilization. Addition of 2 mole percent yields $\approx$ 20 % increase, 5 mole percent yields $\approx$ 50 % increase, and 10 mole percent yields $\approx$ 100 % increase. In the range of concentrations measured, it appears that each mole of αTocQ vaguely contributes $\approx$ 10 % increase in scattering.

Both T_m and r provide information on the melting behaviour of the samples, but it is important to consider that both parameters are influenced by the assignment of a zero-contrast condition at high temperature (i.e. the assumption of ideal lateral mixing of samples at 55 °C), which is supported by both FRET and DSC techniques. We define a depression in the melting point T_m with the addition of any tocopherol or tocopherylquinone and a broadening of the transition which is captured by a decrease in the rate parameter r. Notably, though the addition of vitamin E can both increase or decrease phase separation, it appears that in any situation, the domains become more susceptible to thermally-driven lipid mixing. Hence, domains may become larger or more compositionally homogeneous (increase in scattering), but their formation and disassembly may be less cooperative. Though we emphasize that while these are not explicitly thermodynamic parameters, the depression in melting point observed by neutron scattering is accurately reflected in our calorimetric data (Fig. 3), though it is unclear if the transition is broadened.

Samples were measured along a heating trajectory to capture the process of domain melting. A subsequent cycle of measurements in a cooling trajectory provided insight to potential artifactual immiscibility and as an assessment of lipid oxidation over the duration of the experiment.[45,62] As illustrated in Fig. 6, total scattering of both the base composition as well as the addition of $\chi_{\alpha Toc} = 0.1$ showed minimal hysteresis, with temperature-point Pearson correlation coefficients > 0.99 and are significant within the uncertainty provided by the accuracy of temperature stage. We note that the subsequent cooling trajectory of the composition containing $\chi_{\alpha Toc} = 0.1$ displayed slightly higher scattering which could be indicative of systematic error in temperature, or of slight sample oxidation. This degree of variability is substantially lower than what would be anticipated for sample oxidation based on studies by Tsubone et al., and as such, we justify that effects from both hysteresis and oxidation are not significant within measurement error.[45] Additionally, the sample returned to null scattering upon re-heating to 55 °C which supports that a laterally homogeneous vesicle was measured.

Parallels to previous work and physiological implications

In our previous work,[39] we began to explore the role of vitamin E in membrane organization using a well established lipid mixture that forms high line tension hemispherical domains owing to the disparity between the saturated and unsaturated homoacyl lipids.[42] The former composition resides near the middle of a two-phase L_o/L_d phase coexistence regime,[77] and as such, the domains from this composition are anticipated to be more resistant to perturbation based on the Lever rule. In this membrane environment, we determined that low concentrations of αToc or γToc do not significantly alter the extent of phase separation, but higher concentrations ($\chi = 0.10$) are able to disrupt domain formation. In contrast, αTocQ slightly promoted phase separation at all concentrations. By comparing our current findings, we can expand our understanding of vitamin E in differing membrane environments

The morphology of ordered domains is a product of a range of forces competing with

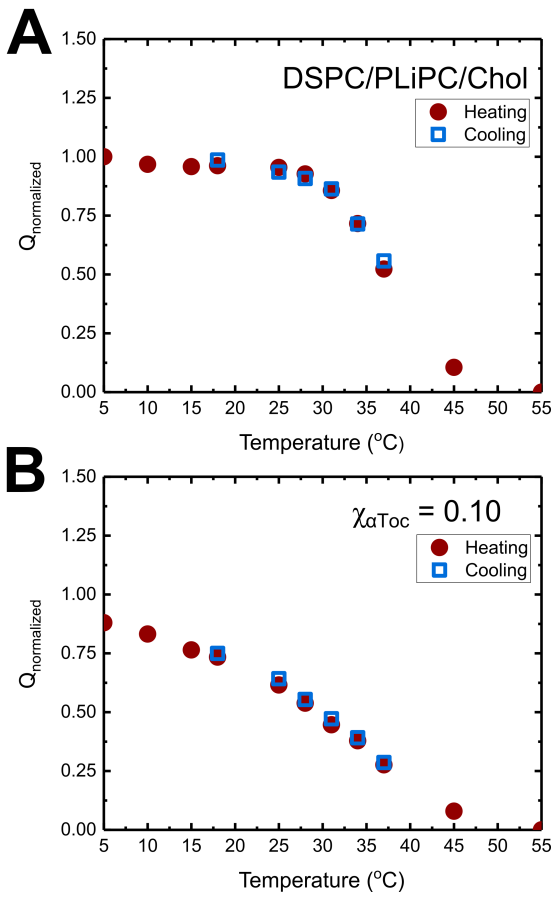

Figure 6: Heating (red circles) and cooling (blue squares) trajectories of (A) DSPC/PLiPC/Chol and (B) the composition with $\chi_{\alpha Toc} = 0.10$ demonstrating no evidence of hysteresis through the phase transition.

line tension, which drives coalescence to larger domains.[42,50] In contrast, the composition introduced here employs a low-melting hybrid lipid (heteroacyl) which may compete against line tension through a variety of mechanisms to favour the formation of nanodomains.[40] The presence of nanodomains suggests a significant competing interaction to those minimizing line tension, and as such, perturbations will likely be more evident in this composition. In addition, the composition used here includes an oxidation-sensitive PUFA lipid which is proposed to interact more preferentially with the tocopherol species.[15–17]

From contrast-matched small-angle neutron scattering, it is evident that high concentrations (χ=0.1) of tocopherol decrease domain stability and promote lipid mixing, regardless of isoform. This observation is consistent with our previous work as well as with experi-

ments by Yang et al. and simulations by Muddana et al. that demonstrate a linactant-like association of αToc with domain boundaries at high concentrations.[39,41,78] In each instance, the linactant effect is observed in compositions with high line tension, and it is unclear if this association is recapitulated in the DSPC/PLiPC/Chol system here, as tocopherols are suspected to preferentially associate with the disordered PUFA phase due to the inherent disorder of the phytyl tail.[15–17]

Low concentrations (χ=0.02) of αToc and γToc, albeit an order of magnitude higher than physiological,[24] induce minimal influence on domain behaviour, which propagates the hypothesis that tocopherols do not dictate lateral organization in biological systems. As the concentration is increased to 5 mole percent, both tocopherols studied here slightly increase lipid clustering —a result not obvious in our previous work. It's possible that this increase is a consequence hindering a lineactant mechanism potentially by competition with the hybrid-acyl PLiPC lipid, or by a greater preference of tocopherol for PUFA environments that isolates tocopherol away from domain boundaries.

Antagonistically, the addition of the oxidized product of vitamin E, αTocQ, induces a dramatic increase in lipid clustering. Within the concentration range studied here, additional αTocQ results in a nearly proportional increase in phase separation. This effect is substantially more pronounced than results in a non-hybrid, non-PUFA lipid composition where no concentration dependence was observed. Interestingly, similarities in domain promoting behaviour exist between αTocQ and the solubility driven influence of the PUFA docosahexanoic acid.[63,79] An aversion of αTocQ for cholesterol-rich phases could provide an explanation for the observed promotion of phase separation.

At the physiological level, these membrane perturbations are suspected to be largely buffered by the critical composition of the biological system. However, these behaviours may become significant if high local concentrations of vitamin E are achieved. As little is understood about the dynamics of membrane protection by vitamin E, it is enticing to speculate how these properties could play into a membrane-protective role.

Volinsky et al. showed that membrane oxidation promotes the formation of raft-like domains in membrane systems.[44,45] As such, oxidized lipid and oxidized tocopherol (αTocQ) induce a very similar effect on lateral lipid organization. Importantly, modifications of raft behaviour have been identified as potential signals to recruit proteins for repair of oxidative damage.[45,80,81] This change in membrane environment creates a two-phased mechanism for tocopherol to be recruited to the site of oxidation as a means to suppress raft formation and quench radical propagation. In this way, phase behaviour can be an unexplored facet of an antioxidant mechanism of vitamin E.

Conclusion

Tocopherols are thought to be the choice antioxidant defence for eukaryotic lipid membranes,[10] but many questions remain on the mechanistic intricacies of their actions as well as additional roles in homeostasis. One such aspect that remains loosely defined is the influence that tocopherols have on the function of the cell membranes in which it resides. In this study, we benchmark a complex oxygen-sensitive ternary lipid composition that displays behaviour reminiscent of nanoscale domains and examine how varieties of vitamin E affect this phase behaviour. FRET, DSC, and contrast-matched SANS support that the base composition exhibits phase coexistence below $\approx$ 46 °C. Addition of small amounts ($\chi = 0.02$) of either α- or γToc have very minor effects on the presence of these PUFA-lipid containing domains. In fact, it is possible that phase separation is slightly promoted. Addition of tocopherol at orders of magnitudes greater than physiological concentrations ($\chi = 0.1$) is able to destabilize domains in a way that is consistent with a linactant behaviour. Uniquely, the oxidized product of αToc (αTocQ) significantly promotes phase separation at all concentrations studied. The current study is qualitatively consistent with our previous work, which scrutinizes the ability of tocopherol to modulate phase behaviour on a physiological scale. Moreover, studying the behaviour of tocopherol in a system with PUFA-lipid domains yields

insight to the intricacies of tocopherol membrane partitioning which may influence its ability to modulate line tension, and could suggest a signalling role for vitamin E in response to membrane oxidation.

Acknowledgement

We acknowledge the support of the National Institute of Standards and Technology, U.S. Department of Commerce in providing access to the VSANS instrument through the Center for High Resolution Neutron Scattering, a partnership between the National Science Foundation and the National Institute of Standards and Technology under Agreement DMR-1508249. M.D. is a recipient of a Canadian Institutes for Health Research (CIHR) CGS-D award and M.H.L.N is a recipient of a Natural Sciences and Engineering Research Council of Canada (NSERC) CGS-D award. S.C. is a recipient of an Ontario Graduate Scholarship. D.M. acknowledges the support of NSERC, [funding reference number RGPIN-2018-04841] and the University of Windsor start-up funds. Certain trade names and company products are identified in order to specify adequately the experimental procedures. Such endorsement does not imply recommendation or endorsement by the National Institute of Standards and Technology, no does it imply that the products are necessarily best for the purpose.

References

(1) Evans, H. M.; Bishop, K. S. On the existence of a hitherto unrecognized dietary factor essential for reproduction. *Science* **1922**, *56*, 650–651.

(2) Atkinson, J.; Marquardt, D.; DiPasquale, M.; Harroun, T. From fat to bilayers: Understanding where and how vitamin E works. *Free Radical Biology and Medicine* **2021**, *176*, 73–79.

(3) Niki, E. Lipid oxidation that is, and is not, inhibited by vitamin E: Consideration

about physiological functions of vitamin E. *Free Radical Biology and Medicine* **2021**, *176*, 1–15.

(4) Azzi, A. Reflections on a century of vitamin E research: Looking at the past with an eye on the future. *Free Radical Biology and Medicine* **2021**, *175*, 155–160.

(5) Brigelius-Flohé, R. Vitamin E research: Past, now and future. *Free Radical Biology and Medicine* **2021**, *177*, 381–390.

(6) Kayden, H. J.; Traber, M. G. Absorption, lipoprotein transport, and regulation of plasma concentrations of vitamin E in humans. *Journal of Lipid Research* **1993**, *34*, 343–358.

(7) Traber, M. G. Vitamin E Regulatory Mechanism. *Annual Review of Nutrition* **2007**, *27*, 347–362.

(8) Dietary Reference Intakes for Vitamin C, Vitamin E, Selenium, and Carotenoids. 2000.

(9) Burton, G. W.; Ingold, K. U. Vitamin E: application of the principles of physical organic chemistry to the exploration of its structure and function. *Accounts of Chemical Research* **1986**, *19*, 194–201.

(10) Traber, M. G.; Atkinson, J. Vitamin E, antioxidant and nothing more. *Free Radical Biology & Medicine* **2007**, *43*, 4–15.

(11) Niki, E. Role of vitamin E as a lipid-soluble peroxyl radical scavenger: in vitro and in vivo evidence. *Free Radical Biology and Medicine* **2014**, *66*, 3–12.

(12) Leng, X.; Kinnun, J. J.; Marquardt, D.; Ghefli, M.; Kučerka, N.; Katsaras, J.; Atkinson, J.; Harroun, T. A.; Feller, S. E.; Wassall, S. R. α-Tocopherol Is Well Designed to Protect Polyunsaturated Phospholipids: MD Simulations. *Biophysical Journal* **2015**, *109*, 1608–1618.

(13) Marquardt, D.; Williams, J. A.; Kučerka, N.; Atkinson, J.; Wassall, S. R.; Katsaras, J.; Harroun, T. A. Tocopherol activity correlates with its location in a membrane: A new perspective on the antioxidant vitamin E. *Journal of the American Chemical Society* **2013**, *135*, 7523–7533.

(14) Harris, P. L.; Embree, N. D. Quantitative Consideration of the Effect of Polyunsaturated Fatty Acid Content of the Diet Upon the Requirements for Vitamin E. *The American Journal of Clinical Nutrition* **1963**, *13*, 385–392.

(15) Williams, J. A.; LoCascio, D. S.; Tsamaloukas, A.; Heerklotz, H.; Stillwell, W.; Wassall, S. R. Preferential Interaction of α-tocopherol with PUFA-containing Lipids Characterized by Isothermal Titration Calorimetry. *Biophysical Journal* **2009**, *96*, 608a.

(16) Atkinson, J.; Harroun, T.; Wassall, S. R.; Stillwell, W.; Katsaras, J. The location and behavior of α-tocopherol in membranes. *Molecular Nutrition & Food Research* **2010**, *54*, 641–651.

(17) DiPasquale, M.; Nguyen, M. H. L.; Pabst, G.; Marquardt, D. Partial Volumes of Phosphatidylcholines and Vitamin E: α-Tocopherol Prefers Disordered Membranes. *The Journal of Physical Chemistry B* **0**, *0*, null, PMID: 36027485.

(18) Marquardt, D.; Williams, J. J., Justin A. Kinnun; Kučerka, N.; Atkinson, J.; Wassall, S. R.; Katsaras, J.; Harroun, T. A. Dimyristoyl Phosphatidylcholine: A Remarkable Exception to α-Tocopherol's Membrane Presence. *Journal of the American Chemical Society* **2014**, *136*, 203–210.

(19) Traber, M. G.; Stevens, J. F. Vitamins C and E: Beneficial effects from a mechanistic perspective. *Free Radical Biology and Medicine* **2011**, *51*, 1000–1013.

(20) Marquardt, D.; Kučerka, N.; Katsaras, J.; Harroun, T. A. α-Tocopherol's Location in Membranes Is Not Affected by Their Composition. *Langmuir* **2015**, *31*, 4464–4472.

(21) Liebler, D. C. The Role of Metabolism in the Antioxidant Function of Vitamin E. *Critical Reviews in Toxicology* **1993**, *23*, 147–169, PMID: 8329114.

(22) Azzi, A. Molecular mechanism of alpha-tocopherol action. *Free Radicals Biol. Med.* **2007**, *43*, 16–21.

(23) Brigelius-Flohé, R.; Galli, F. Vitamin E: A vitamin still awaiting the detection of its biological function. *Molecular Nutrition and Food Research* **2010**, *54*, 583–587.

(24) Atkinson, J.; Epand, R. F.; Epand, R. M. Tocopherols and tocotrienols in membranes: A critical review. *Free Radical Biology and Medicine* **2008**, *44*, 739–764.

(25) Dillard, C. J.; Gavino, V. C.; Tappel, A. L. Relative Antioxidant Effectiveness of α-Tocopherol and γ-Tocopherol in Iron-Loaded Rats. *The Journal of Nutrition* **1983**, *113*, 2266–2273.

(26) Kono, N.; Ohto, U.; Hiramatsu, T.; Urabe, M.; Uchida, Y.; Satow, Y.; Arai, H. Impaired A-TTP-PIPs Interaction Underlies Familial Vitamin E Deficiency. *Science* **2013**, *340*, 1106–1110.

(27) Sesso, H. D.; Buring, J. E.; Christen, W. G.; Kurth, T.; Belanger, C.; MacFadyen, J.; Bubes, V.; Manson, J. E.; Glynn, R. J.; Gaziano, J. M. Vitamins E and C in the Prevention of Cardiovascular Disease in Men: The Physicians' Health Study II Randomized Controlled Trial. *Journal of the American Medical Association* **2008**, *300*, 2123–2133.

(28) Gysin, R.; Azzi, A.; Visarius, T. γ-Tocopherol inhibits human cancer cell cycle progression and cell proliferation by down-regulation of cyclins. *The FASEB Journal* **2002**, *16*, 1952–1954.

(29) Lippman, S. M. et al. Effect of Selenium and Vitamin E on Risk of Prostate Cancer and Other Cancers. *Jama* **2009**, *301*, 39.

(30) Klein, E. A. et al. Vitamin E and the risk of prostate cancer: The selenium and vitamin E cancer prevention trial (SELECT). *JAMA - Journal of the American Medical Association* **2011**, *306*, 1549–1556.

(31) Yang, C. S.; Suh, N.; Kong, A. N. T. Does vitamin E prevent or promote cancer? *Cancer Prevention Research* **2012**, *5*, 701–705.

(32) Li, Y. C.; Park, M. J.; Ye, S. K.; Kim, C. W.; Kim, Y. N. Elevated levels of cholesterol-rich lipid rafts in cancer cells are correlated with apoptosis sensitivity induced by cholesterol-depleting agents. *American Journal of Pathology* **2006**, *168*, 1107–1118.

(33) Simons, K.; Ikonen, E. Functional Rafts in Cell Membranes. *Nature* **1997**, *387*, 569–572.

(34) Simons, K.; Gerl, M. J. Revitalizing membrane rafts: New tools and insights. *Nature Reviews Molecular Cell Biology* **2010**, *11*, 688–699.

(35) Lingwood, D.; Simons, K. Lipid Rafts As a Membrane-Organizing Principle. *Science* **2010**, *327*, 46–50.

(36) Bratton, B. A.; Maly, I. V.; Hofmann, W. A. Effect of polyunsaturated fatty acids on proliferation and survival of prostate cancer cells. *PLOS ONE* **2019**, *14*, e0219822.

(37) Gu, Z.; Wu, J.; Wang, S.; Suburu, J.; Chen, H.; Thomas, M. J.; Shi, L.; Edwards, I. J.; Berquin, I. M.; Chen, Y. Q. Polyunsaturated fatty acids affect the localization and signaling of PIP3/AKT in prostate cancer cells. *Carcinogenesis* **2013**, *34*, 1968–1975.

(38) Hanson, S.; Thorpe, G.; Winstanley, L.; Abdelhamid, A. S.; Hooper, L. Omega-3, omega-6 and total dietary polyunsaturated fat on cancer incidence: systematic review and meta-analysis of randomized trials. *British Journal of Cancer* **2020**, 1260–1270.

(39) DiPasquale, M.; Nguyen, M. H.; Rickeard, B. W.; Cesca, N.; Tannous, C.; Castillo, S. R.; Katsaras, J.; Kelley, E. G.; Heberle, F. A.; Marquardt, D. The an-

tioxidant vitamin E as a membrane raft modulator: Tocopherols do not abolish lipid domains. *Biochimica et Biophysica Acta (BBA) - Biomembranes* **2020**, *1862*, 183189.

(40) Heberle, F. A.; Petruzielo, R. S.; Pan, J.; Drazba, P.; Kučerka, N.; Standaert, R. F.; Feigenson, G. W.; Katsaras, J. Bilayer Thickness Mismatch Controls Domain Size in Model Membranes. *J. Am. Chem. Soc.* **2013**, *135*, 6853–6859.

(41) Muddana, H. S.; Chiang, H. H.; Butler, P. J. Tuning membrane phase separation using nonlipid amphiphiles. *Biophysical Journal* **2012**, *102*, 489–497.

(42) García-Sáez, A. J.; Chiantia, S.; Schwille, P. Effect of line tension on the lateral organization of lipid membranes. *Journal of Biological Chemistry* **2007**, *282*, 33537–33544.

(43) Jacob, R. F.; Mason, R. P. Lipid Peroxidation Induces Cholesterol Domain Formation in Model Membranes*. *Journal of Biological Chemistry* **2005**, *280*, 39380–39387.

(44) Volinsky, R.; Paananen, R.; Kinnunen, P. K. J. Oxidized Phosphatidylcholines Promote Phase Separation of Cholesterol-Sphingomyelin Domains. *Biophysical Journal* **2012**, *103*, 247–254.

(45) Tsubone, T. M.; Junqueira, H. C.; Baptista, M. S.; Itri, R. Contrasting roles of oxidized lipids in modulating membrane microdomains. *Biochimica et Biophysica Acta (BBA) - Biomembranes* **2019**, *1861*, 660–669.

(46) Sharma, P.; Varma, R.; Sarasij, R.; Ira,; Gousset, K.; Krishnamoorthy, G.; Rao, M.; Mayor, S. Nanoscale organization of multiple GPI-anchored proteins in living cell membranes. *Cell* **2004**, *116*, 577–589.

(47) Plowman, S. J.; Muncke, C.; Parton, R. G.; Hancock, J. F. H-ras, K-ras, and inner plasma membrane raft proteins operate in nanoclusters with differential dependence on the actin cytoskeleton. *Proceedings of the National Academy of Sciences* **2005**, *102*, 15500–15505.

(48) Levental, I.; Veatch, S. L. The Continuing Mystery of Lipid Rafts. *Journal of Molecular Biology* **2016**, *428*, 4749–4764, Molecular Biology of Membrane Lipids.

(49) Heberle, F. A.; Doktorova, M.; Scott, H. L.; Skinkle, A. D.; Waxham, M. N.; Levental, I. Direct label-free imaging of nanodomains in biomimetic and biological membranes by cryogenic electron microscopy. *Proceedings of the National Academy of Sciences* **2020**, *117*, 19943–19952.

(50) Heberle, F. A.; Doktorova, M.; Goh, S. L.; Standaert, R. F.; Katsaras, J.; Feigenson, G. W. Hybrid and nonhybrid lipids exert common effects on membrane raft size and morphology. *Journal of the American Chemical Society* **2013**, *135*, 14932–14935.

(51) Buboltz, J. T.; Feigenson, G. W. A novel strategy for the preparation of liposomes: rapid solvent exchange. *Biochimica et Biophysica Acta (BBA) - Biomembranes* **1999**, *1417*, 232–245.

(52) Petruzielo, R. S.; Heberle, F. A.; Drazba, P.; Katsaras, J.; Feigenson, G. W. Phase behavior and domain size in sphingomyelin-containing lipid bilayers. *Biochimica et Biophysica Acta - Biomembranes* **2013**, *1828*, 1302–1313.

(53) Ferreira, E. B.; Lima, M. L.; Zanotto, E. D. DSC Method for Determining the Liquidus Temperature of Glass-Forming Systems. *Journal of the American Ceramic Society* **2010**, *93*, 3757–3763.

(54) Pencer, J.; Mills, T.; Anghel, V.; Kreuger, S.; Epand, R. M.; Katsaras, J. Detection of submicron-sized raft-like domains in membranes by small-angle neutron scattering. *The European Physical Journal E* **2005**, *18*, 447–458.

(55) DiPasquale, M.; Nguyen, M. H. L.; Castillo, S. R.; Heberle, F. A.; Marquardt, D. In *Membrane Lipids: Methods and Protocols*; Cranfield, C. G., Ed.; Springer US: New York, NY, 2022; pp 163–177.

(56) Marquardt, D.; Heberle, F. A.; Nickels, J. D.; Pabst, G.; Katsaras, J. On scattered waves and lipid domains: detecting membrane rafts with X-rays and neutrons. *Soft Matter* **2015**, *11*, 9055–9072.

(57) Barker, J.; Moyer, J.; Kline, S.; Jensen, G.; Cook, J.; Gagnon, C.; Kelley, E.; Chabot, J. P.; Maliszewskyj, N.; Parikh, C.; Chen, W.; Murphy, R. P.; Glinka, C. The very small angle neutron scattering instrument at the National Institute of Standards and Technology. *Journal of Applied Crystallography* **2022**, *55*, 271–283.

(58) Nguyen, M. H. L.; DiPasquale, M.; Rickeard, B. W.; Yip, C. G.; Greco, K. N.; Kelley, E. G.; Marquardt, D. Time-resolved SANS reveals pore-forming peptides cause rapid lipid reorganization. *New J. Chem.* **2021**, *45*, 447–456.

(59) R., K. S. Reduction and analysis of SANS and USANS data using IGOR Pro. *Journal of Applied Crystallography* **2006**, *39*, 895–900.

(60) Glatter, O.; Kratky, O. *Small Angle X-Ray Scattering*; Academic Press: New York, 1982.

(61) Pencer, J.; Anghel, V. N.; Kučerka, N.; Katsaras, J. Scattering from laterally heterogeneous vesicles. I. Model-independent analysis. *Journal of Applied Crystallography* **2006**, *39*, 791–796.

(62) Konyakhina, T. M.; Feigenson, G. W. Phase diagram of a polyunsaturated lipid mixture: Brain sphingomyelin/1-stearoyl-2-docosahexaenoyl-sn-glycero-3-phosphocholine/cholesterol. *Biochimica et Biophysica Acta (BBA) - Biomembranes* **2016**, *1858*, 153–161.

(63) Wassall, S. R.; Stillwell, W. Polyunsaturated fatty acid-cholesterol interactions: Domain formation in membranes. *Biochimica et Biophysica Acta - Biomembranes* **2009**, *1788*, 24–32.

(64) Marquardt, D.; Heberle, F. A.; Greathouse, D. V.; Koeppe, R. E.; Standaert, R. F.; Van Oosten, B. J.; Harroun, T. A.; Kinnun, J. J.; Williams, J. A.; Wassall, S. R.; Katsaras, J. Lipid bilayer thickness determines cholesterol's location in model membranes. *Soft Matter* **2016**, *12*, 9417–9428.

(65) Konyakhina, T. M.; Wu, J.; Mastroianni, J. D.; Heberle, F. A.; Feigenson, G. W. Phase diagram of a 4-component lipid mixture: DSPC/DOPC/POPC/chol. *Biochim. Biophys. Acta* **2013**, *1828*, 2204–2214.

(66) Feigenson, G. W.; Buboltz, J. T. Ternary phase diagram of dipalmitoyl-PC/dilauroyl-PC/cholesterol: Nanoscopic domain formation driven by cholesterol. *Biophysical Journal* **2001**, *80*, 2775–2788.

(67) Buboltz, J. T. Steady-state probe-partitioning fluorescence resonance energy transfer: A simple and robust tool for the study of membrane phase behavior. *Phys. Rev. E* **2007**, *76*, 021903.

(68) Koynova, R.; Caffrey, M. Phases and phase transitions of the phosphatidylcholines. *Biochimica et Biophysica Acta (BBA) - Reviews on Biomembranes* **1998**, *1376*, 91–145.

(69) Taylor, G. J.; Heberle, F. A.; Seinfeld, J. S.; Katsaras, J.; Collier, C. P.; Sarles, S. A. Capacitive Detection of Low-Enthalpy, Higher-Order Phase Transitions in Synthetic and Natural Composition Lipid Membranes. *Langmuir* **2017**, *33*, 10016–10026.

(70) Ortiz, A.; Aranda, F. J.; Gómez-Fernández, J. C. A differential scanning calorimetry study of the interaction of α-tocopherol with mixtures of phospholipids. *Biochimica et Biophysica Acta (BBA) - Biomembranes* **1987**, *898*, 214–222.

(71) Massey, J. B.; She, H. S.; Pownall, H. J. Interaction of vitamin E with saturated phospholipid bilayers. *Biochemical and Biophysical Research Communications* **1982**, *106*, 842–847.

(72) Wassall, S. R.; Thewalt, J. L.; Wong, L.; Gorrissen, H.; Cushley, R. J. Deuterium NMR study of the interaction of α-tocopherol with a phospholipid model membrane. *Biochemistry* **1986**, *25*, 319–326.

(73) Sánchez-Migallón, M. P.; Aranda, F. J.; Gómez-Fernández, J. C. Interaction between α-tocopherol and heteroacid phosphatidylcholines with different amounts of unsaturation. *Biochimica et Biophysica Acta (BBA) - Biomembranes* **1996**, *1279*, 251–258.

(74) Demel, R.; De Kruyff, B. The function of sterols in membranes. *Biochimica et Biophysica Acta (BBA) - Reviews on Biomembranes* **1976**, *457*, 109–132.

(75) Tristram-Nagle, S.; Nagle, J. F. Lipid bilayers: thermodynamics, structure, fluctuations, and interactions. *Chemistry and Physics of Lipids* **2004**, *127*, 3–14.

(76) Ririe, K. M.; Rasmussen, R. P.; Wittwer, C. T. Product Differentiation by Analysis of DNA Melting Curves during the Polymerase Chain Reaction. *Analytical Biochemistry* **1997**, *245*, 154–160.

(77) Veatch, S. L.; Keller, S. L. Separation of Liquid Phases in Giant Vesicles of Ternary Mixtures of Phospholipids and Cholesterol. *Biophysical Journal* **2003**, *85*, 3074–3083.

(78) Yang, S.-T.; Kiessling, V.; Tamm, L. K. Line tension at lipid phase boundaries as driving force for HIV fusion peptide-mediated fusion. *Nature Communications* **2016**, *7*, 11401.

(79) Wassall, S. R.; Stillwell, W. Docosahexaenoic acid domains: the ultimate non-raft membrane domain. *Chem. Phys. Lipids* **2008**, *153*, 57–63.

(80) Volinsky, R.; Kinnunen, P. K. J. Oxidized phosphatidylcholines in membrane-level cellular signaling: from biophysics to physiology and molecular pathology. *The FEBS Journal* **2013**, *280*, 2806–2816.

(81) Zampagni, M.; Evangelisti, E.; Cascella, R.; Liguri, G.; Becatti, M.; Pensalfini, A.; Uberti, D.; Cenini, G.; Memo, M.; Bagnoli, S.; Nacmias, B.; Sorbi, S.; Cecchi, C. Lipid rafts are primary mediators of amyloid oxidative attack on plasma membrane. *Journal of Molecular Medicine* **2010**, *88*, 597–608.

TOC Graphic

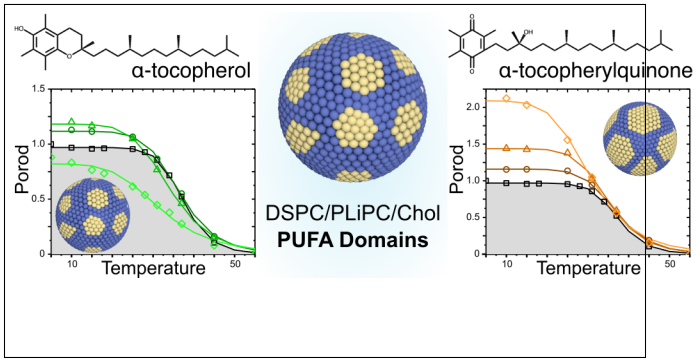
α-tocopherol
Porod
Temperature
DSPC/PLiPC/Chol
PUFA Domains
α-tocopherylquinone
Porod
Temperature